



# NIH Public Access

## Author Manuscript

*Biochemistry*. Author manuscript; available in PMC 2014 September 24.

Published in final edited form as:  
*Biochemistry*. 2013 September 24; 52(38): . doi:10.1021/bi400647c.

## The topology of the yeast Ras converting enzyme as inferred from cysteine accessibility studies

**Emily R. Hildebrandt, Dillon M. Davis, John Deaton, Ranjith K. Krishnankutty, Edward Lilla, and Walter K. Schmidt**

Department of Biochemistry and Molecular Biology, The University of Georgia, Athens, GA 30602, USA

### Abstract

The Ras converting enzyme (Rce1p) is an endoprotease that is involved in the post-translational processing of the Ras GTPases and other isoprenylated proteins. Its role in Ras biosynthesis marks Rce1p as an anti-cancer target. By assessing the chemical accessibility of cysteine residues substituted throughout the *S. cerevisiae* Rce1p sequence, we have determined that yeast Rce1p has eight segments that are protected from chemical modification. Notably, the three residues that are essential for yeast Rce1p function (E156, H194 and H248) are all chemically inaccessible and associated with separate protected segments. By specifically assessing the chemical reactivity and glycosylation potential of the NH<sub>2</sub> and COOH termini of Rce1p, we further demonstrate that Rce1p has an odd number of transmembrane spans. Substantial evidence is presented that the most NH<sub>2</sub>-terminal segment functions as a transmembrane segment with the extreme NH<sub>2</sub> terminus projecting into the ER lumen. Because each of the remaining seven segments is of insufficient length to contain two spans and is flanked by chemically reactive positions, we infer that these segments are not transmembrane segments but rather represent compact structural features and/or hydrophobic loops that penetrate but do not fully span the bilayer (i.e. re-entrant helices). We thus propose a topological model in which yeast Rce1p contains a single transmembrane helix localized at its extreme NH<sub>2</sub>-terminus and one or more re-entrant helices and/or compact structural domains that populate the cytosolic face of the ER membrane. Lastly, we demonstrate that the natural cysteine residues of Rce1p are chemically inaccessible and fully dispensable for *in vivo* enzyme activity, formally eliminating a cysteine-based enzymatic mechanism for this protease.

### Keywords

Protein farnesylation; Post-translational modification; Ras; Membrane enzymes; Protease; Rce1p; CaaX protein; cysteine scanning; PEG-Maleimide

The Ras converting enzyme (Rce1p) is required for the proteolytic maturation of a large subset of isoprenylated proteins (1, 2). Relevant biomedical targets of Rce1p include the Ras GTPases. These proteins and other targets are typically referred to as CaaX proteins due to the presence of a COOH-terminal tetrapeptide sequence (cysteine, aliphatic, aliphatic, one of several amino acids) that serves as a recognition motif for isoprenylation. Rce1p is responsible for removal of the aaX portion of the motif subsequent to isoprenylation. Proteolysis is followed by carboxylmethylation of the COOH-terminal isoprenylated

\*corresponding author: Walter K. Schmidt, 706-583-8241 (phone), 706-542-1738 (fax), wschmidt@bmb.uga.edu.

Supplemental Information

Table S1 contains a complete list of the low and multi-copy plasmids encoding cysteine substitution mutants of Rce1p Cys0. Table S2 contains detailed hydrophyt analyses of wildtype yeast Rce1p using 16 different prediction methods and compares it to the PEG-mal data. Supporting materials may be accessed free of charge online at <http://pubs.acs.org>.

cysteine. In some instances, CaaX proteins undergo additional modification involving S-acylation (e.g. N and H-Ras) or proteolysis (e.g. prelamin A and yeast **a**-factor precursor). The above post-translational modifications modulate the membrane partitioning and protein-protein interaction properties of CaaX proteins, and interfering with these steps is considered having anti-cancer therapeutic value.

Rce1p is a membrane protein that is localized to the endoplasmic reticulum (ER) membrane (3, 4). It has not yet been purified in active form, and its three-dimensional structure remains undetermined. Hydropathy analyses predict it to be an integral membrane protein with multiple membrane spanning segments (i.e. polytopic), ranging from 6-10 spans depending on the algorithm used (5) (Table S2). A polytopic protease is unusual but not without precedent. Notable examples include Ste24p with which Rce1p has partially overlapping activity, the presenilins that cleave the precursor of the A<sub>β</sub> peptide and Notch, the signal peptide peptidase (SPP) and related SPP-family members, the Site 2 protease (S2P) that is involved in the proteolytic liberation of membrane anchored transcription factors, and Rhomboid that regulates a range of activities, including production of a cell signaling factor, parasite invasion, mitochondrial homeostasis, and potentially bacterial quorum sensing (6, 7). Although hydropathy analysis consistently identifies Rce1p as being a membrane protein, it is important to note that hydropathy algorithms only identify hydrophobic stretches within proteins. These algorithms do not distinguish between bitopic (fully transmembrane) and monotopic orientation (a hydrophobic loop that dips into and out of one leaflet of the bilayer; also called a re-entrant helix). The results of this study suggest that Rce1p likely has both types of hydrophobic segments.

The catalytic mechanism of Rce1p has also eluded classification, with cysteine and metalloprotease mechanisms being most often cited and a novel mechanism even being possible (5, 8, 9). Three residues (a glutamate and two histidines) have been identified that are conserved among Rce1p orthologs, including those from prokaryotic species (10, 11). These residues are required for the activity of yeast and trypanosomal Rce1p, suggesting that they are part of the Rce1p active-site (5, 12). As part of an active-site, these residues are hypothesized to lie within the interfacial region between the ER membrane and cytosol where interaction with isoprenylated proteins would be expected. To test this hypothesis, we performed a careful topological study of yeast Rce1p, primarily using a membrane impermeant PEGylated sulfhydryl modifying agent (i.e. PEG-Maleimide 5000; PEG-Mal) to probe the accessibility of naturally occurring or introduced cysteine residues (13, 14). We complement these studies with an assessment of the glycosylation potential of the NH<sub>2</sub> and COOH terminal ends of Rce1p, and also provide hydropathy analyses of Rce1p and related orthologs. The inferred topology localizes the essential residues to the cytoplasmic side of the membrane bilayer, as expected.

## Materials and Methods

### Media and yeast strains

Strains were routinely cultured using liquid or solid synthetic complete dropout media (e.g. YEPD, SC-Ura, SC-Ura-His + 6 mM histidinol) at 30 °C. Histidinol supplemented plates were prepared by adding 6 mM histidinol (Sigma-Aldrich) to SC-Ura-His media after the sterilized media had cooled to approximately 60 °C. Sty50 (*MATa trp1 leu2 ura3 his4 suc2::LEU2*) was used to assess glycosylation status and histidine auxotrophy (15). Multi-copy (2 $μ$ ) plasmid-transformed variants of EG123 (*MATa trp1 leu2 ura3 his4 can1*) were used for isolation of membranes used for cysteine accessibility studies (16). Low copy (*CEN*) plasmid-transformed variants of SM3614 (*MATa trp1 leu2 ura3 his4 can1 ste24::LEU2 rce1::TRP1*) were used to assess the function of Rce1p mutants against tester strains IH1793 (*MAT lys1*) and RC757 (*MAT sst2-1 rme his6 met1 can1 cyh2*) (16, 17).

Plasmid-bearing versions of strains were created using standard methods as previously described (18).

## Plasmids

All plasmids used in this study are listed in Tables 1 and S1. Plasmids were generally constructed using standard approaches, and all new mutants were verified by sequencing the entire *RCE1* open reading frame.

pWS499 (*CEN URA3 P<sub>TPI</sub>-RCE1(1-30)-HA-SUC2-HIS4c*), a multi-copy vector encoding *RCE1* (1-30) fused to *HA-SUC2-HIS4C*, was created by replacing the *OST4* portion in pJK90 with *RCE1* (1-30) using recombination-based cloning methods after linearization of pJK90 with *SmaI* (19).

pWS787 (*CEN URA3 RCE1-HA Cys0*), a low-copy vector that encodes HA-tagged cysteine-less Rce1p, was created by iterative application of the QuikChange™ method and appropriate mutagenic primers. The starting point for this plasmid construction was pWS398 (*CEN URA3 RCE1-HA C251A*) (5). Re-introduction of individual cysteine residues was also typically by the QuikChange™ method. These low-copy vectors were generally converted to multi-copy vectors by ligation-based subcloning, typically involving a *XhoI*-*NotI* fragment from the parent vector ligated into the same sites of pRS426 (*2μ URA3*).

Certain plasmid constructions involved direct subcloning from pre-existing plasmids. For example, pWS954 and pWS955 were created by subcloning a *BamHI*-*NotI* fragment encoding the cysteine-free HA tag from pWS787 into the same sites of pWS108 (*CEN URA3 RCE1-HA*) or pWS404 (*2μ URA3 RCE1-HA*). pWS934 (*2μ URA3 P<sub>PGK</sub> His<sub>10</sub>-HA<sub>N</sub>-RCE1 Cys0*) was constructed by recombination-based cloning using the larger *BsABI*-*SphI* fragment of pWS127 and smaller *BglIII*-*PflMI* fragment of pWS787. pWS127 (*2μ URA3 P<sub>PGK</sub> His<sub>10</sub>-HA<sub>N</sub>-RCE1 L177I*) was also cloned by recombination-based methods using a PCR product derived from pSM1275 (*CEN URA3 RCE1*) and a *BglIII*-*AatII* gapped pSM1282 (*2μ URA3 P<sub>PGK</sub> His<sub>10</sub>-HA<sub>N</sub>-STE24*).

Several plasmids were constructed that encode Rce1p with an altered NH<sub>2</sub>-terminus. pWS1119 (*CEN URA3 RCE1-HA<sub>C</sub> MACAA*) encodes amino acids AACAA inserted after the start codon and was created by QuikChange™ using pWS108 as the parent vector; pWS1121 is the *Cys0* multi-copy version. pWS1110 (*CEN URA3 RCE1-HA<sub>C</sub> 1-41*) was created by recombination-based methods using synthetic paired oligonucleotides designed to gap repair pWS492 digested with *NheI* such that the desired sequence would be removed. pWS1146 (*CEN URA3 His<sub>10</sub>-HA<sub>N</sub>-RCE1*) encodes an NH<sub>2</sub>-terminal His<sub>10</sub>-HA tag that was created by recombination-based methods using a PCR product derived from pWS127 and *EcoRI* gapped pWS100.

Tag-less versions of Rce1p (pWS1130, pWS1131 and pWS1158) were constructed by *BglIII* digestion and re-ligation of the HA<sub>C</sub>-tagged version. This process removes the HA-tag but leaves an Asp-Leu extension at the COOH-terminus. pWS1162 encodes amino acids VNDTG inserted after the start codon followed by a doubly iterated HA epitope. This plasmid was created by recombination-based cloning using a DNA fragment encoding the VNDTG sequence and *AatII* digested pWS1146; the VNDTG fragment was produced by annealing and extending partially overlapping complementary oligos. pWS1163 encodes a doubly iterated HA epitope followed by VNDTG at the COOH-terminus. It was also created by recombination-based methods using *BamHI* digested pWS108 and overlapping oligos that were extended.

## Yeast a-factor production assays

Rce1p mutants were evaluated for function using a genetic assay that relies on Rce1p-dependent **a**-factor production (5). The assay involves the mixing of *MATa* cells expressing a Rce1p variant with *MAT*<sup>+</sup> cells, followed by selection for diploid cells that form as a consequence of fusion between the cells of opposite mating type. Yeast used for the test were first cultured to saturation in appropriate selective media then diluted with fresh media to 1.0 OD<sub>600</sub>. The diluted *MAT*<sup>+</sup> cell suspension was loaded into multiple wells of a 96-well plate (90 µl/well), into which diluted *MATa* cell suspensions were added (10 µl/well) to form initial mating mixtures. A volume of each mixture (10 µl) was transferred to a fresh well containing the *MAT*<sup>+</sup> cell suspension (90 µl/well). The transfer was repeated iteratively to prepare a range of diluted *MATa* cells in the background of excess *MAT*<sup>+</sup> cells. The set of mating mixtures prepared for each *MATa* strain was spotted onto an SD plate, and the formation of diploid colonies scored after 2-3 days of growth at 30 °C. The serial dilutions were also spotted onto SC-Lys plates to confirm that the input amounts of *MATa* cells were similar across the strains evaluated; these plates allow the selective growth of *MATa* haploid cells and diploid cells that may have formed during the processing of the samples.

The **a**-factor mating pheromone produced by yeast expressing Rce1p-HA or Rce1p-HA (Cys0) was isolated according to published methods (20, 21). In brief, yeast were cultured to saturation for 36 hours at 30 °C in polypropylene tubes, the tubes washed extensively with water, and the secreted **a**-factor that had adhered to the tube was recovered by washing the tube wall with methanol. The samples were concentrated by speed-vac, resuspended in 50 µl of DMSO, and prepared as 2-fold serial dilutions in YEPD that were spotted onto a lawn of RC757. The formation of a spot in the lawn is indicative of the presence of pheromone in the sample. The relative potency of pheromone can be determined by comparing the activity pattern of the serial diluted sample against that of a positive control.

## Membrane preparation

Yeast membranes enriched for Rce1p were isolated according to previously published methods with some modifications (12, 22). In all cases, yeast were cultured to 1.0 OD<sub>600</sub> in SC-Ura, harvested (3000g × 5 min), washed with cold 10 mM sodium azide, and re-isolated by centrifugation prior to preparation of membranes.

For recovery of intact membranes, cells were incubated on ice for 15 minutes with Tris/DTT buffer (100 mM Tris, pH 9.6 with HCl, 10 mM DTT), harvested by centrifugation, and treated with Zymolyase 100T (Cape Cod Inc., East Falmouth, MA) for 60 minutes at 30 °C in buffer Z (50 mM KPi pH 7.5, 1.4 M sorbitol, 10 mM NaN<sub>3</sub>) containing 2 µg Zymolyase per ml of original culture. Resulting spheroplasts were washed once in Buffer Z, resuspended in Buffer S (0.3 M sorbitol, 50 mM HEPES pH 7.4, 2 mM EDTA, 1 mM EGTA) containing protease inhibitors (1 mM phenylmethylsulfonyl fluoride, 1 µg/ml each aprotinin, leupeptin, pepstatin, chymostatin), and lysed by dounce homogenization. The lysate was subjected to centrifugation (1000g × 10 min) to generate a partly clarified supernatant from which membranes were then recovered (16,000g × 60 min). The isolated membranes were washed with Buffer S, reisolated by centrifugation, and carefully resuspended into Buffer S before storage at -80 °C. The protein concentrations of the membrane suspensions were determined by a BioRad assay.

For recovery of fractured membranes, cells were directly lysed into Buffer M (0.3 M mannitol, 50 mM HEPES pH 7.4, 2 mM EDTA, 1 mM EGTA) containing protease inhibitors (as described above). Cell suspensions containing 1 part cells, 2 parts buffer, and 1 part silica beads were vortexed vigorously (4 min at 4 °C), chilled on ice for 2 min, and the cycle repeated until 16 min of total vortexing time was achieved. Membranes were

recovered from the lysates by centrifugation as described above except that the membranes were washed and resuspended with Buffer M.

### Endo H sensitivity assay

Protein extracts were prepared from mid-log yeast via alkaline hydrolysis in the presence of 2-mercaptoethanol (me) according to previously published methods (23). The protein pellet recovered after trichloroacetic acid (TCA) precipitation was washed with cold acetone and resuspended in Endo H sample buffer (50 mM Tris, pH 6.8 with HCl, 10% glycerol, 2% SDS, 5% me, 0.5 mM EDTA, 0.0025% bromophenol blue) containing protease inhibitors as described above. The lysates were used to assemble reactions with Endo Hf according to manufacturer's instructions (New England Biolabs).

### PEG-Maleimide (PEG-Mal) treatment and detection

Membranes were diluted to 0.3 mg/ml with Buffer S or Buffer M (50 µl final) as appropriate and treated with or without 1 mM mono-methyl PEG 5000 maleimide (PEG-Mal; Sigma-Aldrich) in the absence and presence of detergent (1% SDS or 0.5% Triton X-100, as specified). After a 1 hr incubation on ice, the reactions were incubated with me (300 mM final) for an additional 10 min to quench reactions; SDS treated samples were incubated at room temperature throughout to prevent precipitation of detergent. Samples were diluted with 2× sample buffer (75 mM Tris at pH 6.8, 24% w/v sucrose, 6% w/v SDS, 3% me, 0.01% bromophenol blue), subjected to 10% or 15% SDS-PAGE, transferred to nitrocellulose membranes, and blots probed with anti-HA (1:10,000) and anti-Kar2p antibodies (1:10,000) according to standard methods; 10% gels were used for Suc2-His4c samples, and 15% gels were used for Rce1p samples. For N-ethylmaleimide (NEM) experiments, membranes were treated with 5 mM NEM (Sigma-Aldrich) for 30 min at room temperature, washed 5 times with Buffer S, and resuspended in Buffer S prior to PEG-Mal addition. Immunoblots used anti-HA monoclonal antibody or anti-RCE polyclonal antibody specific to amino acids 24-42 (3). Prestained molecular weight protein standards used were BenchMark (Invitrogen/Novex) or PageRuler (ThermoScientific).

### Hydropathy and multiple sequence alignment analyses

The sequences of Rce1p orthologs from *S. cerevisiae*, *H. sapiens*, *C. elegans*, *A. thaliana*, *S. pombe*, *T. brucei*, and *D. melanogaster* were aligned using Clustal Omega (<http://www.clustal.org/omega/>) and additionally evaluated using the MEMSAT-SVM server (<http://bioinf.cs.ucl.ac.uk/psipred/>) with default settings. Gap adjustments placed by Clustal Omega within predicted transmembrane helices were manually repositioned to just lie outside the nearest edge of the predicted segment in order to preserve an uninterrupted sequence for the segment. The protein sequence of *S. cerevisiae* Rce1p was also evaluated using a suite of publically available hydropathy analysis programs (Table S2). These included: DAS (24); HMMTOP (25); MINNOU (26); MPEX (27); OCTOPUS (28); PHDhtm (29); PolyPhobius (30); PredictProtein (31); SOSUI (32); TM-COFFEE (33); TMHMM (34); TMpred (35); TOPCONS (36); TopPred (37).

## Results

### Reporters for monitoring the integrity and orientation of microsomes derived from yeast ER membranes

Several lines of evidence identify yeast Rce1p as a membrane-associated protein, including hydropathy analysis, recovery of activity with particulate fractions, and localization to the endoplasmic reticulum (ER) (3). Topology predictions suggest multiple potential transmembrane segments varying in number and relative placement depending on the

algorithm (Table S2) (5). Bioinformatic alignment of Rce1p homologs further suggests that proposed active-site residues are localized to separate hydrophobic segments (10, 11). To evaluate the accuracy of these topological predictions, we have used PEG-Mal 5000 as a membrane impermeant chemical probe to map the accessibility of sulphydryl moieties found naturally in or added to the yeast Rce1p sequence while in the context of its native membrane environment.

Our approach first required the identification of experimental conditions allowing for recovery of ER-derived microsomes that are properly oriented and impermeant to the probe (i.e. right side in and retaining membrane integrity). We investigated these properties using three proteins having distinct topologies (Figure 1A). Two contain the dual Suc2-His4c topology reporter cassette (38). The third protein is Kar2p, a well-established soluble protein of the yeast ER lumen.

The orientation of a membrane protein created by fusion of Ost4p and the dual Suc2p-His4c reporter cassette has been previously described as having an inward facing NH<sub>2</sub>-terminus (i.e. in the ER-lumen) and a cytosolically oriented reporter cassette, leading to histidine prototrophy and absence of glycosylation (38). We have reproduced these observations using our conditions optimized for recovery of intact microsomes (Figure 1B and 1C, respectively). The second protein that we evaluated (R1-30) is based on the fusion of the first 30 amino acids of yeast Rce1p, which is predicted to contain a transmembrane segment, and the dual reporter cassette. Fortunately, evaluation of R1-30 indicated an orientation opposite to that of the Ost4p-based fusion as judged by its ability to be glycosylated and inability to confer histidine prototrophy on histidinol-containing media. The proposed transmembrane segment of the R1-30 fusion was not cleaved by the action of the signal peptidase as inferred by retention of the fusion with a particulate fraction after treatment with sodium carbonate (see Fig. 5C). These results are consistent with the R1-30-based fusion having a non-cleaved transmembrane segment and a cytosolic facing NH<sub>2</sub>-terminus.

The Suc2-His4c reporter has multiple cysteine residues available for chemical modification with PEG-Mal (Figure 1D). This reagent adds ~5 kDa of mass per modified cysteine to a target, leading to a size shift when monitored by SDS-PAGE and immunoblotting. In the context of intact yeast microsomes containing the Ost4p or R1-30-based fusions, we determined that the Ost4-fusion was chemically reactive with PEG-Mal, while R1-30 was unreactive (Figure 1E). Moreover, we observed that the soluble ER luminal protein Kar2p, which has a single cysteine, was also protected from PEG-Mal modification (Figure 1F). Disrupting the microsomes with detergent made all three proteins available for modification. In the presence of detergent, the Kar2p population was only partly modified suggesting that its cysteine remains partly inaccessible under the tested conditions. This observation has been previously reported (39).

It is important to note that the methods used for isolation of microsomes can impact membrane integrity. Surveying several buffers and cell lysis methods, we identified dounce-based lysis of spheroplasts into sorbitol-containing buffer as the best method for isolation of intact microsomes. By contrast, bead-based mechanical breakage of yeast cells into mannitol-containing buffer yielded compromised microsomes (see Figure 4B).

### **The natural cysteine residues of Rce1p are dispensable for in vivo activity and inaccessible to PEG-Mal in vitro**

We sought to investigate the topology of full-length yeast Rce1p by mapping its chemical reactivity to PEG-Mal. Several HA-tagged Rce1p variants were evaluated. Wild-type Rce1p- with a COOH-terminal HA tag (HA<sub>C</sub>) contains eight cysteine residues (Cys8): seven natural cysteine residues (amino acids 105, 114, 217, 243, 244, 251 and 286) plus one

additional cysteine that is part of the triply iterated HA-tag cassette (amino acid 354). The PEG-Mal modification profile of Cys8 revealed that at least one cysteine was accessible to the chemical probe (Figure 2A, Cys8). In the presence of the detergent Triton X-100 (TX), multiple cysteine residues were modified, yielding a ladder of modified species. The use of SDS further enhanced chemical reactivity, yielding a species that was heavily modified and difficult to resolve by SDS-PAGE. An Rce1p variant lacking the cysteine associated with the HA epitope (Cys7) was unreactive with PEG-Mal unless membrane integrity was compromised (Figure 2A, Cys7). Over-exposure of the immunoblot for Cys7 reacted with PEG-Mal in the presence of Triton X-100 further revealed a ladder of 7 PEGylated species. A reverse order of addition experiment in which Cys7 was pretreated with membrane permeant me prior to addition of PEG-Mal revealed no modification in either the absence or presence of SDS. This result indicates that me fully quenches the concentration of PEG-Mal used in our experiment. Furthermore, this result disallows the possibility that PEG-Mal modification occurs on latent cysteine reactive sites during the processing of the sample (i.e. cystine bonds are reduced upon dilution of membranes with SDS-PAGE sample buffer). Collectively, these results suggest that the HA tag is disposed toward the cytosol, that the natural cysteine residues of Rce1p are not involved in disulfide bonds, and that the natural cysteines are all inaccessible to chemical modification. Inaccessibility is presumably due to the residues being membrane embedded, located in the ER lumen, or buried within a tightly folded cytosolic domain. A functional truncated version of Rce1p (Cys7 1-277) was also modified by PEG-Mal, indicating that the HA-tag after amino acid 277 is also in the cytosol. As a control, a cysteine-less variant of Rce1p (Cys0) was evaluated. As predicted, no mass shifts were detected upon treatment with PEG-Mal in the absence or presence of detergent (Figure 2A, Cys0). The lack of chemical reactivity of Cys0 establishes that PEG-Mal modification of Rce1p is entirely cysteine dependent.

Using Cys0 as a starting point, we evaluated the effect of introducing a single cysteine at various locations on the protein. For placement of a cysteine at the ends of Rce1p, the Cys0 variant was modified to have a cysteine-containing HA tag at either the NH<sub>2</sub> or COOH-terminus (Cys1 HA<sub>N</sub> and Cys1 HA<sub>C</sub>, respectively). Evaluation of these species revealed that Cys1 HA<sub>N</sub> was protected against PEG-Mal modification while Cys1 HA<sub>C</sub> was reactive (Figure 2A; Cys1 HA<sub>N</sub> and Cys1 HA<sub>C</sub>, respectively). In both cases, PEG-Mal modification in the presence of detergent produced a single modified species as predicted. Taken together, these results indicate that the COOH-terminus of Rce1p is cytosolic, while the NH<sub>2</sub>-terminus is luminal, within the membrane, or protected by tightly folded structure.

An important concern for our study involves the impact of added epitopes and mutations on the overall folding of Rce1p. We have previously documented that a COOH-terminal HA-epitope and certain mutations do not impact Rce1p activity as judged by an *in vivo* genetic test designed to monitor Rce1p-dependent production of the yeast **a**-factor mating pheromone (5). We interpret these observations to indicate that Rce1p is properly folded in these instances. Previously, we had documented that C251 is not essential for yeast Rce1p activity, despite a reported claim to the contrary (5, 9). The impact of lost cysteine content on Rce1p function, however, had not been previously assessed. Our results with Cys0 and Cys1 variants indicate that the natural cysteine residues of Rce1p are dispensable for its function *in vivo* as assessed by a genetic test for production of yeast **a**-factor (Figure 2B). Using a second test that more directly quantifies the amount of **a**-factor produced by yeast, we determined that the Cys0 expressing strain produces **a**-factor at an amount 41% ± 4 relative to Cys8. This result is consistent with our observation that Cys0 steady state levels are approximately 30% that of Cys8 (Hildebrandt and Schmidt, unpublished observation), suggesting that the reduced ability of Cys0 to produce **a**-factor is not due to activity differences but expression differences. The reason for the reduced expression of Cys0

remains unknown. Our observation that cysteine-free Rce1p is functional thus conclusively eliminates the possibility that Rce1p has a catalytic cysteine at any position.

### Functional evaluation of substituted cysteine mutants

The observation that Rce1p lacking cysteine content is functional was fortuitous as this allowed us to use the Cys0 species as a background to examine the accessibility of single cysteine residues reintroduced throughout the sequence. The cysteines were reintroduced at various locations, including predicted loops and hydrophobic segments. When available, a natural serine residue was targeted to minimize potentially negative impacts on enzyme activity. The proposed active-site residues were also targeted. The entire collection of mutants was evaluated for function using our genetic assay under conditions of relatively low expression so as not overlook mutants with subtle effects on activity. Our analysis revealed that most substitutions were innocuous (Figure 3A). A few cysteine substitution mutants, however, compromised activity. As expected, complete loss of activity was observed when cysteine substituted for a previously identified essential amino acid (E156, H194 and H248) (5). Loss of activity was also observed for F234C and S162C in the context of Cys0 but not in the context of wild-type Rce1p (i.e. Cys8, Figure 3B). Reduced activity was observed for I82C, L169C, and S260C. Immunoblot analysis revealed that both the inactive and reduced activity mutants were expressed at levels similar to the active mutants (see Figure 4). We interpret the reduced function of these mutants to reflect the additive effect of the eight mutations present in these proteins. The inactive and reduced activity mutants were subsequently evaluated with PEG-Mal, but the results obtained with these mutants should be interpreted with caution due to the possibility that functional defects might be associated with aberrant folding and possibly altered topology.

### Chemical reactivity of substituted cysteine residues

To assess the chemical reactivity of the lone cysteine residue within the Rce1p variants that were created, ER-derived microsomes were isolated and treated with PEG-Mal. Microsomes were prepared in one of two ways. Intact microsomes were recovered from a dounce-based lysate of spheroplasts (Figure 4A) while microsomes with compromised integrity were recovered from a lysate prepared by mechanical agitation in the presence of silica beads (i.e. bead beating) (Figure 4B). Intact microsomes were also evaluated in the presence of the detergent Triton X-100 (Figure 4C). These three conditions were chosen to reflect accessibility of PEG-Mal to distinct regions of a membrane protein. Intact microsomes would allow PEG-Mal accessibility to cytosolically oriented residues, but not those oriented into the ER lumen or residing within the membrane. Compromised microsomes would allow PEG-Mal accessibility to residues oriented either toward the cytosol or lumen, but not to those within the membrane. Detergent treated microsomes would allow for accessibility to cysteine residues independent of location. As a measure for the integrity of the microsomes and effectiveness of the PEG-Mal reagent, the ER luminal protein Kar2p was evaluated in parallel with the Rce1p variants. For intact microsomes, we observed that Kar2p was typically not modified (Figure 4A, top panel). For compromised and detergent-treated microsomes, Kar2p was consistently modified (Figures 4B and 4C, top panels).

PEG-Mal accessibility studies using intact microsomes revealed that some, but not all, of the cysteine residues evaluated were chemically reactive (Figure 4A, bottom panel). Where chemical reactivity was observed, relative reactivity ranged from weak to strong. In such situations, we infer that increased chemical reactivity correlates to a certain extent with increased solvent exposure of the residue. A general pattern emerged from the analysis. Cysteine residues positioned within the first 10 amino acids of Rce1p were protected from PEG-Mal. This was followed by a chemically reactive region (i.e. positions 24-40). The alternating pattern of a protected region followed by a reactive region was repeated such that

7 protected regions were identified (Figure 4A, see black bars). Within some protected regions, weak reactivity was occasionally observed that was variable between replicates (e.g. positions 61, 96, and 125). The protected regions were scattered throughout the Rce1p sequence: positions 2-10 (9 residues), 51-61 (11 residues), 96-125 (29 residues), 155-169 (15 residues), 187-196 (13 residues), 243-251 (8 residues), and 286-297 (12 residues). Notably, the protected regions contain residues that are essential for Rce1p activity (i.e. positions 156, 194, and 248). As expected, these protected regions also contain naturally occurring cysteine residues (i.e. positions 105, 114, 243, 244, 251, and 286) previously determined to be inaccessible to PEG-Mal (see Figure 2). One natural cysteine (position 217) was not associated, however, with a protected region due to a lack of sufficient coverage around this position. Given the previously established non-reactivity of all the natural cysteine residues of Rce1p with PEG-Mal, we infer that position 217 is associated with an additional eighth protected region that lies somewhere between positions 208 and 233.

To assess whether protected regions were oriented into the lumen of the microsomes, we evaluated their reactivity in the context of compromised microsomes (Figure 4B). As expected, reactivity was observed in association with an NH<sub>2</sub>-terminal HA tag (Cys1 HAN). Across most of the Rce1p variants evaluated, the pattern of PEG-Mal reactivity was essentially unchanged compared to results obtained with intact microsomes. Minor differences in reactivity were within experimental variability that we have observed.

To assess whether protected regions might be embedded in the membrane environment, we evaluated their reactivity in the context of Triton X-100 (Figure 4C). Under this condition, most of the Rce1p variants were reactive with PEG-Mal, including those variants associated with naturally occurring cysteine residues (i.e. positions 243, 244, and 286) and essential residues (i.e. positions 156, 194, and 248). The few exceptions were associated with cysteine residues placed near the NH<sub>2</sub>-terminus (i.e. positions 2, 5, 10, and 51). Positions 2 and 51 were inaccessible to PEG-Mal, while positions 5 and 10 were only weakly modified. Positions 162, 251 and 297 were also substantially less reactive than other residues.

### The NH<sub>2</sub>-terminus of Rce1p has an uncleaved transmembrane segment

We investigated the NH<sub>2</sub>-terminus in more detail because the severely reduced level of PEG-Mal reactivity at multiple positions within the extreme NH<sub>2</sub>-terminus of Rce1p could potentially be explained by cleavage and loss of an NH<sub>2</sub>-terminal signal peptide. The prediction program SignalP4.1 identifies a low probability cleavable signal peptide associated with amino acids 1-21 of Rce1p, and single cysteine mutations of amino acids within the 1-51 region do not reduce this probability (40). At first glance, the presence of a true cleavable signal peptide seems improbable since Cys1 HAN retains PEG-Mal reactivity and can still be detected by immunoblot (see Figure 2). It remained formally possible, however that the addition of an HA tag interferes with the cleavage event, resulting in retention of the HA tag and NH<sub>2</sub>-terminal residues.

Presuming that the NH<sub>2</sub>-terminus was not cleaved, we predicted that cysteine residues within the NH<sub>2</sub>-terminus might be better accessible to PEG-Mal if SDS were used as the detergent since we had observed such an effect in prior experiments. When cysteine residues that were PEG-Mal resistant under Triton X-100 conditions were re-evaluated in the presence of SDS, we observed significantly improved reactivity at position 10 (Figure 5A). The reactivity at position 10 was similar to that observed for nearby positions that were accessible under Triton X-100 conditions (i.e. positions 24, 30, and 40). By comparison, SDS moderately improved reactivity at positions 2 and 5, and weakly improved reactivity at position 51. In addition, we observed that full length R1-30-Suc2p-His4c remains membrane associated in the presence of carbonate, while a large portion of the luminal protein Kar2p is

released (Figure 5C), further demonstrating that a cleaved signal sequence is unlikely at the NH<sub>2</sub>-terminus of Rce1p.

We also re-evaluated the impact of an NH<sub>2</sub>-terminal HA tag on Rce1p activity. While we previously observed that such placement of the tag was apparently without consequence (Figure 2B), it should be noted that our initial evaluation was performed under over-expressing conditions. In yeast, over-expression of a defective protein is sometimes sufficient to rescue its total activity such that a genetic phenotype associated with protein dysfunction is corrected; this is why we performed our genetic test using low-expression plasmids (see Figure 3). Since the NH<sub>2</sub>-termini of Rce1p orthologs vary considerably in content and length at the NH<sub>2</sub>-terminus, an extension of the NH<sub>2</sub>-terminus was not predicted to disrupt activity or alter folding dynamics. Indeed, low expression of Rce1p having an NH<sub>2</sub>-terminal HA tag (Cys8 HA<sub>N</sub>; *CEN*-based plasmid; natural *RCE1* promoter) yielded *in vivo* activity identical to that of untagged and COOH-terminal tagged variants (Figure 5B; Cys7 tag-less and Cys8 HA<sub>C</sub>, respectively).

#### The topological orientations of the NH<sub>2</sub> and COOH-termini of Rce1p are not influenced by the presence of an HA tag

The addition of an HA tag onto a protein could potentially alter its function, localization, or if a membrane protein, its topology. In order to determine whether the HA tag had an effect on the position of the termini of Rce1p, the PEG-Mal reactivity of untagged Rce1p (Cys7 tag-less) was evaluated; the absence of an epitope tag required the use of an anti-Rce1p antibody for protein detection by immunoblot (3). As previously observed, none of the natural cysteine residues were modified in the absence of detergent. Cys7 tag-less was further modified to contain a four amino acid insertion (Ala-Cys-Ala-Ala) after the initiating methionine (Cys8 MACAA) or a cysteine residue as the penultimate COOH-terminal amino acid (Cys8 T314C). These Rce1p variants were fully functional (Figure 5B). Again, all 7 natural cysteine residues were protected against PEG-Mal modification. Consistent with the observed reactivity of the NH<sub>2</sub> and COOH HA-tagged versions of Rce1p, Cys8 MACAA was reactive with PEG-Mal only in the presence of detergent while the Cys8 T314C was reactive in the absence of detergent (Figure 5D).

To independently validate our PEG-Mal observations, we used a glycosylation approach to determine the orientation of the NH<sub>2</sub> and COOH termini of Rce1p. An N-linked glycosylation recognition sequence (i.e. Asn-x-Ser/Thr) was engineered at the extreme NH<sub>2</sub> or COOH-terminus of Rce1p-HA<sub>N</sub> and Rce1p-HA<sub>C</sub>, respectively, such that the most distal HA epitope of the triply iterated tag was replaced with the sequence VNDTG. The glycosylation sequence did not interfere with Rce1p function (Figure 5B, NDT<sub>N</sub> and NDT<sub>C</sub>). The NH<sub>2</sub>-terminal NDT sequence was glycosylated, consistent with it being oriented into the ER lumen. The COOH-terminal NDT sequence was not glycosylated, consistent with it being oriented into the cytosol (Figure 5E).

One possible interpretation of our data is that the NH<sub>2</sub>-terminal transmembrane segment represents the only transmembrane segment of Rce1p. In this case, deletion of the NH<sub>2</sub>-terminus might make Rce1p more readily extractable from membranes. We observed, however, that an Rce1p variant lacking its first 41 amino acids ( 1-41) was not extracted from membranes by salt, urea, or carbonate treatments, but was extracted by SDS (Figure 5F). This profile exactly matched that of wildtype Rce1p (Hildebrandt and Schmidt, unpublished observation). Unlike wildtype Rce1p, the deletion mutant was inactive (Figure 5B, 1-41).

## The essential residues of Rce1p are located within hydrophobic environments

As previously mentioned, the three essential residues of Rce1p map to regions that are protected against PEG-Mal reactivity. To further probe the disposition of these residues, we evaluated whether *N*-ethylmaleimide (NEM), a small, membrane diffusible sulfhydryl modifier, could modify cysteine residues at these positions and protect them from subsequently being modified by PEG-Mal. The chemical reactivity of NEM is such that it is highly reactive in aqueous solvent but much less so in a hydrophobic environment where sulfhydryls poorly ionize (13). This leads to differential blocking of residues depending on location: cytosolic and luminal residues are efficiently blocked by NEM while residues within membranes environs are inefficiently blocked. Under identical reaction conditions, we observed that NEM pretreatment completely protected against PEG-Mal modification when a unique cysteine was positioned at the NH<sub>2</sub> terminus (MACAA) but only partly protected cysteine residues at the positions of essential residues (i.e. positions 156, 194, and 248) (Figure 6). Cysteine residues positioned at 286 and 297 were not blocked by NEM pretreatment. These observations lead us to conclude that the NH<sub>2</sub>-terminus is solvent exposed. Conversely, positions 156, 194, 248, 286, and 297 are solvent protected, albeit to different extents, suggestive that these positions are within a hydrophobic environment.

## Comparison of PEG-Mal data and hydropathy analyses

PEG-Mal analysis identified eight protected regions within yeast Rce1p. We compared this result with the output of hydropathy analyses derived using the yeast Rce1p sequence and a suite of publically available programs developed for identification of transmembrane segments (DAS, HMMTOP, MEMSAT-SVM, MINNOU, MPEX, OCTOPUS, PHDhtm, PolyPhobius, PredictProtein, SOSUI, TM-COFFEE, TMHMM, TMpred, TOPCONS, TopPred) (Table S2). Some of these programs rely on direct analysis of a single input sequence, while others extrapolate a prediction from a multiple sequence alignment. The number of transmembrane segments predicted by these programs ranged from as few as six (TOPCONS) to as many as ten (PolyPhobius). Of the programs evaluated, only MEMSAT-SVM and PredictProtein identified segments that consistently overlapped with those identified through our PEG-Mal studies (Figures 7 and 8A; Table 2). In general, the segments predicted for yeast Rce1p by these two algorithms differed by only a few residues in length or relative position. Notably, the proposed active-site (E156, H194, and H248) and natural cysteine residues of yeast Rce1p (105, 114, 217 243, 244, 251, and 286) all lie within predicted hydrophobic segments. The MEMSAT-SVM and PredictProtein algorithms also provide signal peptide prediction but did not identify a signal peptide for yeast Rce1p.

The eight predicted hydrophobic segments of yeast Rce1p were also predicted for Rce1p orthologs, with the exception of segment I, which was not predicted for worm (*Ce*) or trypanosome (*Tb*) Rce1p. In all cases the relative position of the essential residues consistently mapped within hydrophobic regions. To best visualize this information in the context of our PEG-Mal and glycosylation data, the predicted hydrophobic segments for each individual sequence were mapped onto a Clustal Omega multiple-sequence alignment of Rce1p orthologs (Figure 7).

## Discussion

Rce1p is an ER localized membrane protein. Its three essential residues (E156, H194, H248; yeast sequence) are resistant to PEG-Mal modification and are only moderately reactive with NEM, suggesting that they lie in a protected, hydrophobic environment. Bioinformatic predictions similarly place these residues in the middle of conserved hydrophobic segments (11). Provided that the essential residues form the catalytic center of Rce1p, these findings are consistent with Rce1p having an active site that is buried in the membrane or otherwise

inaccessible to solvent. The presence of a proteolytic active-site within the membrane environment is not without precedent. For the rhomboid protease, the serine-histidine dyad active-site is surrounded by transmembrane helices. For the Ste24p CaaX protease, the active-site lies near the membrane/cytosolic interface at the apex of a large internal cavity (41, 42).

As part of our effort to resolve the topology of yeast Rce1p, we identified eight PEG-Mal protected segments in yeast Rce1p that are independently identifiable through certain hydropathy analyses (i.e. MEMSAT-SVM and PredictProtein). Each of these segments is long enough to span a membrane bilayer (i.e. >15 amino acids). A simple, but dubious, interpretation of our data is that each identified segment correlates with a transmembrane segment of Rce1p (Figure 8B). The strongest argument challenging this topology is our observation that the NH<sub>2</sub> and COOH termini have opposite reactivity to PEG-Mal and differ in N-linked glycosylation potential. Since the termini of Rce1p are on opposite sides of the membrane, Rce1p must have an odd number of spans (i.e. 1, 3, 5 or 7).

For any topology model of Rce1p having an odd number of spans, we propose that it must include a transmembrane segment between amino acids 1 and 24 (i.e. segment I) that is oriented with the NH<sub>2</sub>-terminus pointing into the ER lumen. We arrive at this conclusion based on the following observations. First, we observe that we can engineer the NH<sub>2</sub>-terminus to be N-linked glycosylated. Second, the NH<sub>2</sub>-terminus (e.g. Cys1 HA<sub>N</sub> and MACAA) is only reactive with PEG-Mal when microsomes are compromised. Third, we observe that positions 2, 5 and 10 are highly resistant to PEG-Mal modification, which would be expected if they reside in a membrane environment. By comparison, positions 24, 30 and 40 strongly react with PEG-Mal under conditions of intact microsomes, suggestive that this region is exposed to the cytosol. Finally, we demonstrate that the first 30 amino acids of Rce1p are sufficient for anchoring the Suc2p-His4c topology reporter in the ER membrane. It has not escaped our attention that the transmembrane segment contained within R1-30-Suc2p-His4c adopts a topology opposite that observed in the context of the full Rce1p molecule. It is thus likely that other portions of Rce1p contribute to the final topological orientation of the NH<sub>2</sub>-terminus.

The most parsimonious interpretation of our data is that Rce1p has a single NH<sub>2</sub>-terminal transmembrane segment that is followed by a series of tightly folded cytosolic domains and/or re-entrant helices separated by loops. We arrive at this conclusion through comparison of the PEG-Mal reactivity profiles of Rce1p using intact and fractured microsomes. Use of fractured microsomes did not reveal any latent PEG-Mal reactive positions, other than the extreme NH<sub>2</sub>-terminus, which would be indicative of luminal disposition. This result suggests that each of the solvent exposed loops is on the cytosolic face of the membrane. Because none of the inaccessible segments is long enough to span the membrane twice, the protected segments likely represent tightly folded cytosolic domains or re-entrant helices. This orientation for Rce1p would also partly explain our inability to successfully introduce consensus N-linked glycosylation sites into any region of Rce1p other than the NH<sub>2</sub> terminus.

A model containing an NH<sub>2</sub>-terminal transmembrane anchor and 7 tightly folded cytosolic domains (Figure 8C) is improbable, however, because Rce1p 1-41 is not readily extracted from the membrane by chaotropic agents (e.g. urea, high salt) or carbonate washing. Since proteins anchored by re-entrant helices can resist membrane extraction, one possible explanation for our results is that Rce1p 1-41 is anchored to the membrane via at least one membrane embedded helix (43-47). While an arrangement containing 7 re-entrant helices places the essential amino acids on the same face of the lipid bilayer (Figure 8D-E), any combination of re-entrant helices (up to 7) and tightly folded cytosolic domains can satisfy

our experimental PEG-Mal accessibility data. Based on the predicted activation energy for forming membrane spans, the most likely candidates for tightly folded cytosolic domains rather than re-entrant helices are helices IV, V and VII (Figure 8A).

The substituted cysteine accessibility method is obviously not high resolution and has shortcomings that can affect the accuracy of its predictions. First and foremost is the reliance of the method on mutants. Even biologically active mutants could have a subpopulation of misfolded protein. Mutations associated with intramembrane helix hairpins and re-entrant helices are especially at risk, since subtle changes at the amino acid level are known to lead to alternative topologies for such spans (48, 49). There is also the possibility that PEG-Mal could react with the residues of solvent exposed pockets that deeply penetrate into the membrane. More liberally interpreting our PEG-Mal data, but maintaining the constraint of an odd number of transmembrane spans, it could therefore be possible that Rce1p has a 3, 5 or 7-span configuration. An interesting possible arrangement is one having five transmembrane spans (I, II, III, VI and VIII) and three re-entrant helices (IV, V and VII) (Figure 8F). The spans have high relative probabilities for forming transmembrane helices and are consistently predicted by hydropathy programs (Figure 8A and Table S2). This configuration localizes two of the proposed essential residues (E156, H194) to the membrane edge or a hydrophobic pocket similar to that seen in Rhomboid (50). The third essential residue (H248) is within the luminal face of the membrane bilayer where it could be part of structure that forms the base of the pocket.

The majority of our topology models for Rce1p incorporate re-entrant helices. Re-entrant helices are rare but present on a wide variety of proteins. In certain proteins, re-entrant helices serve as the only membrane-anchoring element (e.g. caveolin, cyclooxygenases, torsinA) (51-53). In other cases, the re-entrant helices are present in addition to transmembrane segments and have a functional role (e.g. aquaporins and ion/small molecule transporters) (54-56). While the Ste24p *CaaX* protease does not have re-entrant helices, Ste24p is similar to Rce1p in that it has an odd number of transmembrane helices and its NH<sub>2</sub> and COOH termini are oriented like that of Rce1p (41, 42). The 7 transmembrane segments of Ste24p form a water-filled  $\beta$ -helical barrel that is situated within the plane of the membrane; this configuration is highly atypical of a transmembrane protein. The Ste14p isoprenylcysteine methyltransferase also lacks re-entrant helices, but it does possess a helix-turn-helix motif that is fully contained within the plane of the membrane and is in essence a longer version of a re-entrant helix (57-59). While the architecture of Ste14p is more consistent with that of a typical membrane protein, it does contain unusual structure features (i.e. a pocket and hydrophobic tunnel) that allow for binding of *S*-adenosyl-L-methionine (co-factor) and farnesylated cysteine (substrate). It will be interesting to eventually determine how the Rce1p structure compares to that of Ste24p and Ste14 and how each independently evolved to bind and interact with isoprenylated substrates.

## Supplementary Material

Refer to Web version on PubMed Central for supplementary material.

## Acknowledgments

We thank the Drs. Lance Wells (University of Georgia), Jeff Brodsky (University of Pittsburgh) and Susan Michaelis (Johns Hopkins Medical) for anti-HA, anti-Kar2p and anti-Rce1p antibodies, respectively. We also thank members of the Schmidt laboratory for critical discussions and technical assistance, especially Samar Aldrugh, Shivan Bhatt and Lisa J. Plummer for plasmid constructions. This work was supported by a grant from the National Institutes of Health (5R01GM067092 to WKS).

## Abbreviations

<b>HEPES</b>	2-[4-(2-hydroxyethyl)piperazin-1-yl]ethanesulfonic acid
<b>me</b>	2-mercaptoethanol
<b>DMSO</b>	dimethyl sulfoxide
<b>DTT</b>	dithiothreitol
<b>ER</b>	endoplasmic reticulum
<b>EDTA</b>	ethylene diamine tetraacetic acid
<b>EGTA</b>	ethylene glycol tetraacetic acid
<b>PEG-Mal</b>	mono-methyl PEG-maleimide 5000
<b>NEM</b>	N-ethylmaleimide
<b>PAGE</b>	polyacrylamide gel electrophoresis
<b>SDS</b>	sodium dodecyl sulfate
<b>TCA</b>	trichloroacetic acid
<b>Tris</b>	tris(hydroxymethyl)aminomethane
<b>TX</b>	Triton X-100

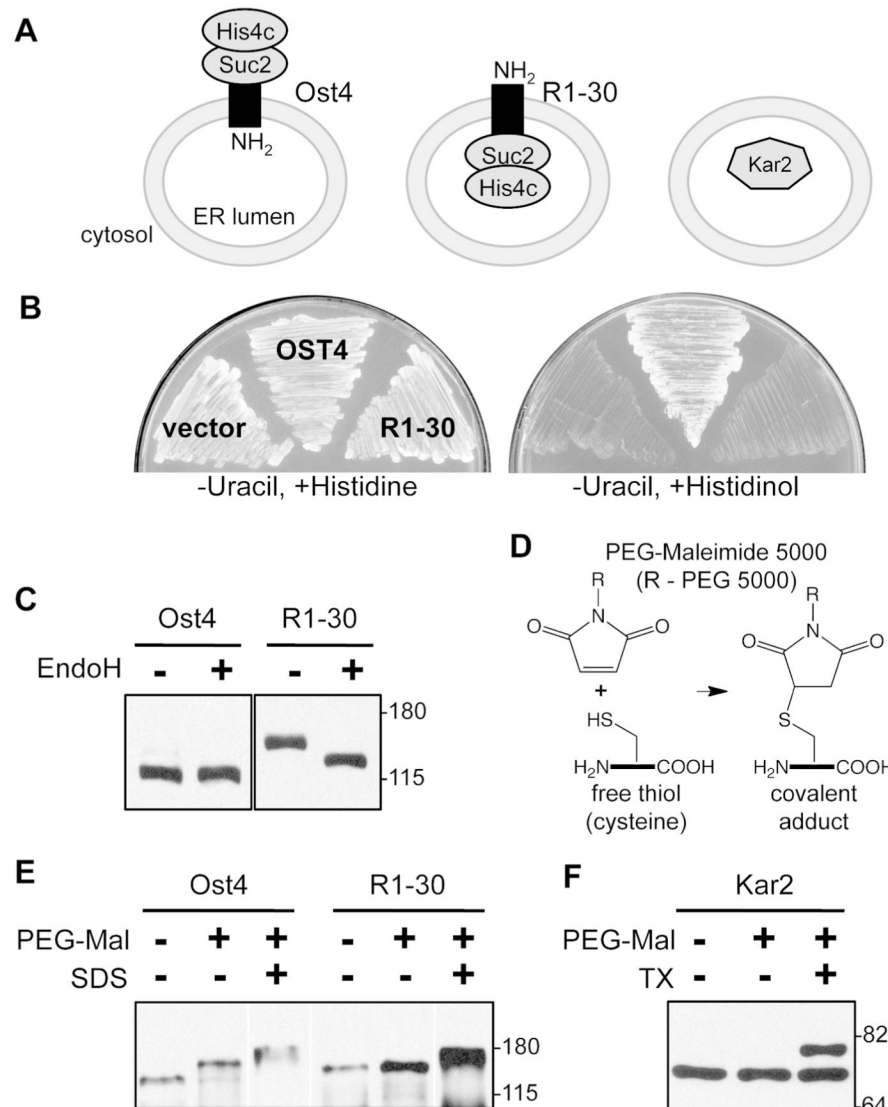
## References

1. Winter-Vann AM, Casey PJ. Post-prenylation-processing enzymes as new targets in oncogenesis. *Nat Rev Cancer.* 2005; 5:405–412. [PubMed: 15864282]
2. Schmidt, W.; Dore, T. The Ras converting enzyme (Rce1p): orthologs, enzymology, and inhibitors. In: Tamanoi; Hrycyna; Bergo, editors. *The Enzymes.* 3rd ed.. Academic Press/Elsevier; 2011. p. 231-258.
3. Schmidt WK, Tam A, Fujimura-Kamada K, Michaelis S. Endoplasmic reticulum membrane localization of Rce1p and Ste24p, yeast proteases involved in carboxyl-terminal CAAX protein processing and amino-terminal a-factor cleavage. *Proc Natl Acad Sci USA.* 1998; 95:11175–11180. [PubMed: 9736709]
4. Bracha-Drori K, Shichrur K, Lubetzky TC, Yalovsky S. Functional analysis of Arabidopsis postprenylation CaaX processing enzymes and their function in subcellular protein targeting. *Plant Physiol.* 2008; 148:119–131. [PubMed: 18641086]
5. Plummer LJ, Hildebrandt ER, Porter SB, Rogers VA, McCracken J, Schmidt WK. Mutational analysis of the ras converting enzyme reveals a requirement for glutamate and histidine residues. *J Biol Chem.* 2006; 281:4596–4605. [PubMed: 16361710]
6. Erez E, Fass D, Bibi E. How intramembrane proteases bury hydrolytic reactions in the membrane. *Nature.* 2009; 459:371–378. [PubMed: 19458713]
7. Urban S, Dickey SW. The rhomboid protease family: a decade of progress on function and mechanism. *Genome Biol.* 2011; 12:231. [PubMed: 22035660]
8. Chen Y, Ma YT, Rando RR. Solubilization, partial purification, and affinity labeling of the membrane-bound isoprenylated protein endoprotease. *Biochemistry.* 1996; 35:3227–3237. [PubMed: 8605158]
9. Dolence JM, Steward LE, Dolence EK, Wong DH, Poulter CD. Studies with recombinant *Saccharomyces cerevisiae* CaaX prenyl protease Rce1p. *Biochemistry.* 2000; 39:4096–4104. [PubMed: 10747800]
10. Pei J, Grishin NV. Type II CAAX prenyl endopeptidases belong to a novel superfamily of putative membrane-bound metalloproteases. *Trends Biochem Sci.* 2001; 26:275–277. [PubMed: 11343912]

11. Pei J, Mitchell DA, Dixon JE, Grishin NV. Expansion of Type II CAAX Proteases Reveals Evolutionary Origin of gamma-Secretase Subunit APH-1. *J Mol Biol*. 2011; 410:18–26. [PubMed: 21570408]
12. Mokry DZ, Manandhar SP, Chicola KA, Santangelo GM, Schmidt WK. Heterologous expression studies of *Saccharomyces cerevisiae* reveal two distinct trypanosomatid CaaX protease activities and identify their potential targets. *Eukaryot Cell*. 2009; 8:1891–1900. [PubMed: 19820121]
13. Lu J, Deutsch C. Pegylation: a method for assessing topological accessibilities in Kv1.3. *Biochemistry*. 2001; 40:13288–13301. [PubMed: 11683639]
14. Bogdanov M, Zhang W, Xie J, Dowhan W. Transmembrane protein topology mapping by the substituted cysteine accessibility method (SCAM(TM)): application to lipid-specific membrane protein topogenesis. *Methods*. 2005; 36:148–171. [PubMed: 15894490]
15. Kim H, Yan Q, Von Heijne G, Caputo GA, Lennarz WJ. Determination of the membrane topology of Ost4p and its subunit interactions in the oligosaccharyltransferase complex in *Saccharomyces cerevisiae*. *Proc Natl Acad Sci U S A*. 2003; 100:7460–7464. [PubMed: 12810948]
16. Michaelis S, Herskowitz I. The **a**-factor pheromone of *Saccharomyces cerevisiae* is essential for mating. *Mol. Cell. Biol.* 1988; 8:1309–1318. [PubMed: 3285180]
17. Tam A, Nouvet F, Fujimura-Kamada K, Slunt H, Sisodia SS, Michaelis S. Dual roles for Ste24p in yeast **a**-factor maturation: NH<sub>2</sub>-terminal proteolysis and COOH-terminal CAAX processing. *J. Cell Biol*. 1998; 142:635–649. [PubMed: 9700155]
18. Elble R. A simple and efficient procedure for transformation of yeasts. *BioTechniques*. 1992; 13:18–20. [PubMed: 1503765]
19. Oldenburg KR, Vo KT, Michaelis S, Paddon C. Recombination-mediated PCR-directed plasmid construction *in vivo* in yeast. *Nucleic Acids Res*. 1997; 25:451–452. [PubMed: 9016579]
20. Nijbroek GL, Michaelis S. Functional assays for the analysis of yeast *ste6* mutants. *Methods Enzymol*. 1998; 292:193–212. [PubMed: 9711555]
21. Kim S, Lapham A, Freedman C, Reed T, Schmidt W. Yeast as a tractable genetic system for functional studies of the insulin-degrading enzyme. *J Biol Chem*. 2005; 280:27481–27490. [PubMed: 15944156]
22. Schmidt WK, Tam A, Michaelis S. Reconstitution of the Ste24p-dependent N-terminal proteolytic step in yeast **a**-factor biogenesis. *J. Biol. Chem.* 2000; 275:6227–6233. [PubMed: 10692417]
23. Fujimura-Kamada K, Nouvet FJ, Michaelis S. A novel membrane-associated metalloprotease, Ste24p, is required for the first step of NH<sub>2</sub>-terminal processing of the yeast **a**-factor precursor. *J. Cell Biol*. 1997; 136:271–285. [PubMed: 9015299]
24. Cserzo M, Wallin E, Simon I, von Heijne G, Elofsson A. Prediction of transmembrane alpha-helices in prokaryotic membrane proteins: the dense alignment surface method. *Protein Eng*. 1997; 10:673–676. [PubMed: 9278280]
25. Tusnady GE, Simon I. Principles governing amino acid composition of integral membrane proteins: application to topology prediction. *Journal of Molecular Biology*. 1998; 283:489–506. [PubMed: 9769220]
26. Cao B, Porollo A, Adamczak R, Jarrell M, Meller J. Enhanced recognition of protein transmembrane domains with prediction-based structural profiles. *Bioinformatics*. 2006; 22:303–309. [PubMed: 16293670]
27. Snider C, Jayasinghe S, Hristova K, White SH. MPEx: a tool for exploring membrane proteins. *Protein Sci*. 2009; 18:2624–2628. [PubMed: 19785006]
28. Viklund H, Elofsson A. OCTOPUS: improving topology prediction by two-track ANN-based preference scores and an extended topological grammar. *Bioinformatics*. 2008; 24:1662–1668. [PubMed: 18474507]
29. Rost B, Sander C. Prediction of protein secondary structure at better than 70% accuracy. *J Mol Biol*. 1993; 232:584–599. [PubMed: 8345525]
30. Kall L, Krogh A, Sonnhammer EL. An HMM posterior decoder for sequence feature prediction that includes homology information. *Bioinformatics*. 2005; 21(Suppl 1):i251–257. [PubMed: 15961464]
31. Rost B, Yachdav G, Liu J. The PredictProtein server. *Nucleic Acids Res*. 2004; 32:W321–326. [PubMed: 15215403]

32. Hirokawa T, Boon-Chieng S, Mitaku S. SOSUI: classification and secondary structure prediction system for membrane proteins. *Bioinformatics*. 1998; 14:378–379. [PubMed: 9632836]
33. Chang JM, Di Tommaso P, Taly JF, Notredame C. Accurate multiple sequence alignment of transmembrane proteins with PSI-Coffee. *BMC Bioinformatics*. 2012; 13(Suppl 4):S1. [PubMed: 22536955]
34. Krogh A, Larsson B, von Heijne G, Sonnhammer EL. Predicting transmembrane protein topology with a hidden Markov model: application to complete genomes. *Journal of Molecular Biology*. 2001; 305:567–580. [PubMed: 11152613]
35. Hofmann K, Stoffel W. TMBase 2 A database of membrane spanning proteins segments. *Biological Chemistry Hoppe-Seyler*. 1993; 374:166.
36. Bernsel A, Viklund H, Hennerdal A, Elofsson A. TOPCONS: consensus prediction of membrane protein topology. *Nucleic Acids Res.* 2009; 37:W465–468. [PubMed: 19429891]
37. Claros MG, von Heijne G. TopPred II: an improved software for membrane protein structure predictions. *Comput Appl Biosci*. 1994; 10:685–686. [PubMed: 7704669]
38. Kim H, Melen K, von Heijne G. Topology models for 37 *Saccharomyces cerevisiae* membrane proteins based on C-terminal reporter fusions and prediction. *J Biol Chem*. 2003; 278:10208–10213. [PubMed: 12524434]
39. Bochud A, Ramachandra N, Conzelmann A. Adaptation of low-resolution methods for the study of yeast microsomal polytopic membrane proteins: a methodological review. *Biochem Soc Trans*. 2013; 41:35–42. [PubMed: 23356255]
40. Petersen TN, Brunak S, von Heijne G, Nielsen H. SignalP 4.0: discriminating signal peptides from transmembrane regions. *Nat Methods*. 2011; 8:785–786. [PubMed: 21959131]
41. Pryor E, Horanyi P, Clark K, Fedorow N, Connelly S, Koszelak-Rosenblum M, Zhu G, Malkowski M, Wiener M, Dumont M. Structure of the integral membrane protein CAAX protease Ste24p. *Science*. 2013; 339:1600–1604. [PubMed: 23539602]
42. Quigley A, Dong Y, Pike A, Dong L, Shrestha L, Berridge G, Stansfeld P, Sansom M, Edwards A, Bounstra C, von Delft F, Bullock A, Burgess-Brown N, Carpenter E. The structural basis of ZMPSTE24dependent laminopathies. *Science*. 2013; 339:1604–1607. [PubMed: 23539603]
43. Dupree P, Parton RG, Raposo G, Kurzchalia TV, Simons K. Caveolae and sorting in the trans-Golgi network of epithelial cells. *EMBO J*. 1993; 12:1597–1605. [PubMed: 8385608]
44. Bickel PE, Scherer PE, Schnitzer JE, Oh P, Lisanti MP, Lodish HF. Flotillin and epidermal surface antigen define a new family of caveolae-associated integral membrane proteins. *J Biol Chem*. 1997; 272:13793–13802. [PubMed: 9153235]
45. Liu Z, Zolkiewska A, Zolkiewski M. Characterization of human torsinA and its dystonia-associated mutant form. *Biochem J*. 2003; 374:117–122. [PubMed: 12780349]
46. Salinas SR, Bianco MI, Barreras M, Ielpi L. Expression, purification and biochemical characterization of GumiI, a monotopic membrane GDP-mannose:glycolipid 42{beta}-D-mannosyltransferase from *Xanthomonas campestris* pv. *campestris*. *Glycobiology*. 2011; 21:903–913. [PubMed: 21367879]
47. Koch J, Brocard C. PEX11 proteins attract Mff and human Fis1 to coordinate peroxisomal fission. *J Cell Sci*. 2012; 125:3813–3826. [PubMed: 22595523]
48. Monne M, Nilsson I, Elofsson A, von Heijne G. Turns in transmembrane helices: determination of the minimal length of a “helical hairpin” and derivation of a fine-grained turn propensity scale. *J Mol Biol*. 1999; 293:807–814. [PubMed: 10543969]
49. Norholm MH, Shulga YV, Aoki S, Epand RM, von Heijne G. Flanking residues help determine whether a hydrophobic segment adopts a monotopic or bitopic topology in the endoplasmic reticulum membrane. *J Biol Chem*. 2011; 286:25284–25290. [PubMed: 21606504]
50. Urban S. Taking the plunge: integrating structural, enzymatic and computational insights into a unified model for membrane-immersed rhomboid proteolysis. *Biochemical Journal*. 2010; 425:501–512. [PubMed: 20070259]
51. Okamoto T, Schlegel A, Scherer PE, Lisanti MP. Caveolins, a family of scaffolding proteins for organizing “preassembled signaling complexes” at the plasma membrane. *J Biol Chem*. 1998; 273:5419–5422. [PubMed: 9488658]

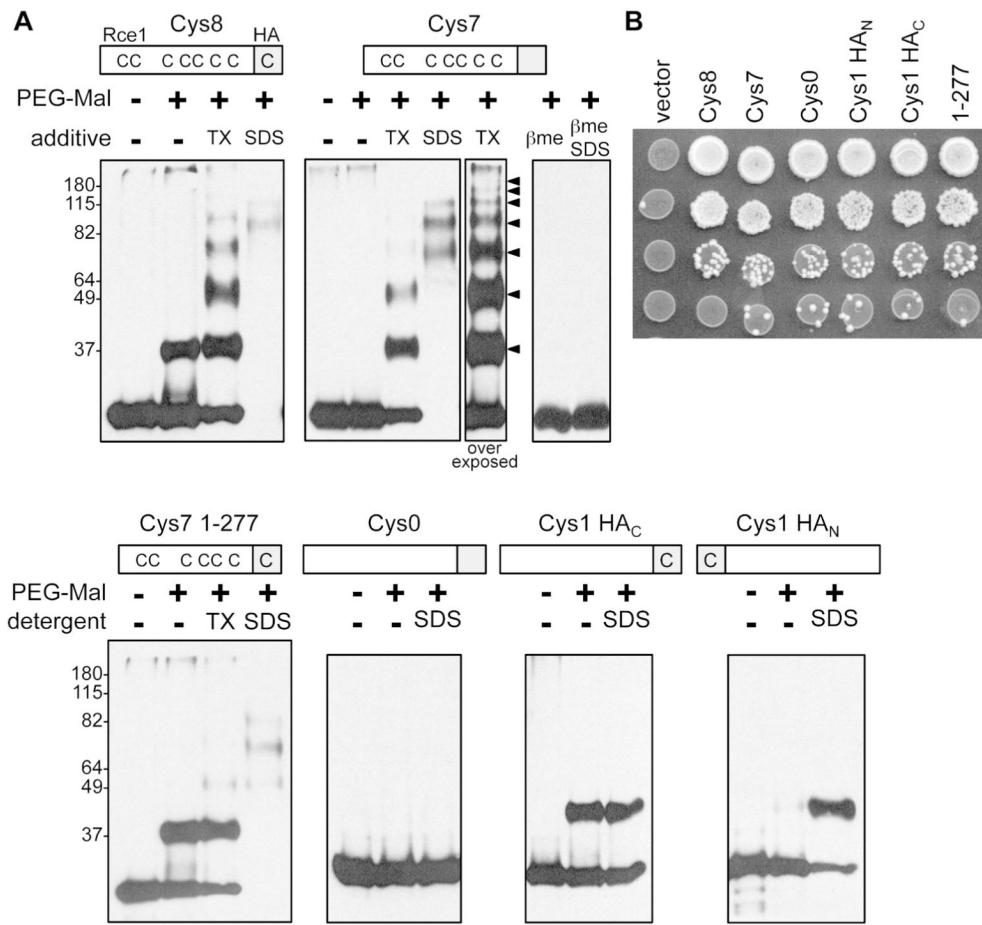
52. Spencer AG, Thuresson E, Otto JC, Song I, Smith T, DeWitt DL, Garavito RM, Smith WL. The membrane binding domains of prostaglandin endoperoxide H synthases 1 and 2. Peptide mapping and mutational analysis. *J Biol Chem.* 1999; 274:32936–32942. [PubMed: 10551860]
53. Vander Heyden AB, Naismith TV, Snapp EL, Hanson PI. Static retention of the luminal monotopic membrane protein torsinA in the endoplasmic reticulum. *EMBO J.* 2011; 30:3217–3231. [PubMed: 21785409]
54. Mitsuoka K, Murata K, Walz T, Hirai T, Agre P, Heymann JB, Engel A, Fujiyoshi Y. The structure of aquaporin21 at 4.52 Å resolution reveals short alpha-helices in the center of the monomer. *Journal of structural biology.* 1999; 128:34–43. [PubMed: 10600556]
55. Iwamoto T, Uehara A, Imanaga I, Shigekawa M. The Na+/Ca<sup>2+</sup> exchanger NCX1 has oppositely oriented reentrant loop domains that contain conserved aspartic acids whose mutation alters its apparent Ca<sup>2+</sup> affinity. *J Biol Chem.* 2000; 275:38571–38580. [PubMed: 10967097]
56. Kanner BI, Borre L. The dual-function glutamate transporters: structure and molecular characterisation of the substrate-binding sites. *Biochim Biophys Acta.* 2002; 1555:92–95. [PubMed: 12206897]
57. Romano JD, Michaelis S. Topological and mutational analysis of *Saccharomyces cerevisiae* Ste14p, founding member of the isoprenylcysteine carboxyl methyltransferase family. *Mol Biol Cell.* 2001; 12:1957–1971. [PubMed: 11451995]
58. Wright LP, Court H, Mor A, Ahearn IM, Casey PJ, Philips MR. Topology of mammalian isoprenylcysteine carboxyl methyltransferase determined in live cells with a fluorescent probe. *Mol Cell Biol.* 2009; 29:1826–1833. [PubMed: 19158273]
59. Yang J, Kulkarni K, Manolaridis I, Zhang Z, Dodd RB, Mas-Droux C, Barford D. Mechanism of isoprenylcysteine carboxyl methylation from the crystal structure of the integral membrane methyltransferase ICMT. *Mol Cell.* 2011; 44:997–1004. [PubMed: 22195972]
60. Sikorski RS, Hieter P. A system of shuttle vectors and yeast host strains designed for efficient manipulation of DNA in *Saccharomyces cerevisiae*. *Genetics.* 1989; 122:19–27. [PubMed: 2659436]
61. Hessa T, Meindl-Beinker NM, Bernsel A, Kim H, Sato Y, Lerch-Bader M, Nilsson I, White SH, von Heijne G. Molecular code for transmembrane-helix recognition by the Sec61 translocon. *Nature.* 2007; 450:1026–1030. [PubMed: 18075582]



**Figure 1. Reporters for assessing the orientation and integrity of microsomes in vitro**

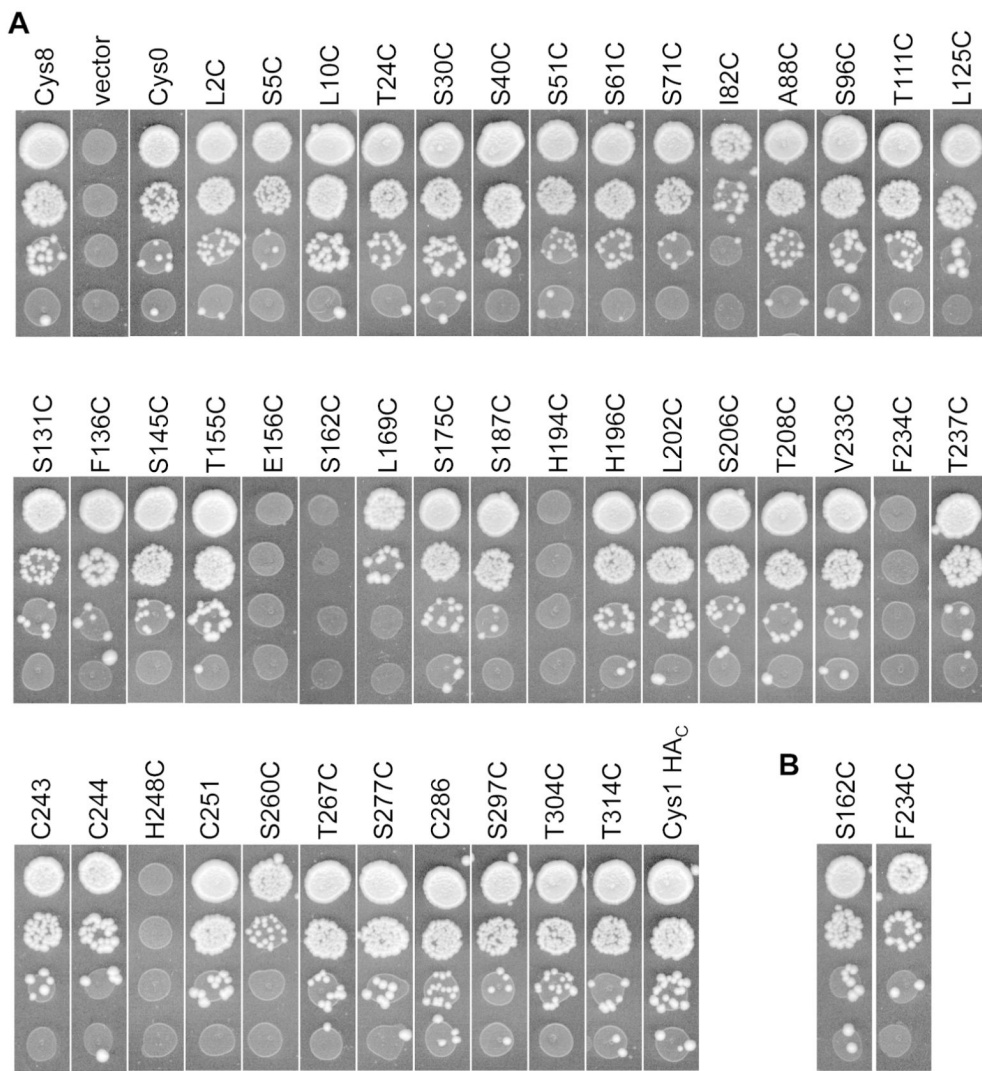
**A)** Cartoon diagrams of reporters used in this study. The Suc2-His4c cassette provides data on the disposition of the cassette. The Suc2 portion is glycosylated only when oriented into the endoplasmic reticulum (ER) lumen. The His4c portion is capable of converting histidinol to histidine only when oriented into the cytosol. The Suc2-His4c fusion also contains an HA epitope tag that lies at the junction between the target protein and cassette. **B)** Sty50 (*his4<sup>L</sup>*) was transformed with plasmids pRS416 (vector), pJK90 (*OST4-HA-SUC2-HIS4c*), or pWS499 (*R1-30-HA-SUC2-HIS4c*). Transformed yeast were struck onto selective media (SC-Ura-His) supplemented with histidine or histidinol as indicated. **C)** Whole cell extracts of yeast shown in **panel B** were prepared, treated with or without EndoH, and analyzed by 10% SDS-PAGE and immunoblotting using the anti-HA antibody. **D)** Chemical reaction associated with PEG-Mal 5000. **E)** Intact microsomes were prepared from yeast strains described in **panel B** and treated with and without PEG-Mal 5000 (~5 kDa) in the absence and presence of 1% SDS. The samples were subsequently analyzed by SDS-PAGE and Western blotting using the anti-HA antibody. The only cysteine residues available for modification lie within the Suc2-His4c cassette (13 total). In this and subsequent data panels

of the same type, numbers next to the panel indicate the relative mobility of kDa protein standards. **F)** Intact microsomes were prepared and analyzed as in **panel E** except that 0.5% Triton X-100 (TX) was used as the detergent and the blot was probed with anti-Kar2p antibody.



**Figure 2. The natural cysteine residues of Rce1p are protected against PEG-mal modification**

**A)** Intact microsomes were prepared from yeast strains expressing the indicated Rce1p variant and processed according to methods described in Figure 1E, except that both SDS and Triton X-100 (TX) were used as detergents and EG123 was used as the yeast strain. Where indicated, Cys7 samples were pre-incubated with  $\beta$ me. The cartoon above each panel indicates the relative position of the triply iterated HA-epitope tag (HA) and the number and relative position of cysteine residues (C) available for modification within the variant. Cys8 has a predicted mass of 40.7 kDa, but migrates approximately 8–10 kDa smaller by SDS-PAGE, as has been previously reported (3). The plasmids used were pWS404 (Cys8), pWS566 (Cys7 1-277), pWS822 (Cys1 HA<sub>C</sub>), pWS823 (Cys0), pWS934 (Cys1 HA<sub>N</sub>), and pWS954 (Cys7). **B)** The plasmids described in **panel A** were transformed into SM3614 and evaluated for their ability to confer mating. The serial dilution mating assay involves preparation of a 10-fold serial dilution of each haploid *MA Ta* strain expressing the indicated Rce1p variant, mixing of the dilution set with an excess of *MAT*<sup>+</sup> yeast (IH1793), and spotting of mixtures onto media selective for diploids.

**Figure 3. Mating profiles of cysteine-substituted Rce1p mutants**

Low-copy plasmids encoding the indicated Rce1p variant behind the natural *RCE1* promoter were introduced into SM3614, and the resultant strains evaluated for their ability to confer yeast mating according to the assay described in Figure 2B. The indicated cysteine substitution mutations were introduced into either **A**) Rce1p Cys0 or **B**) wildtype Rce1p. C243, C244, C251 and C286 are not technically substitution mutations since they are at their natural positions. The plasmids used are described in Tables 1 and S1.

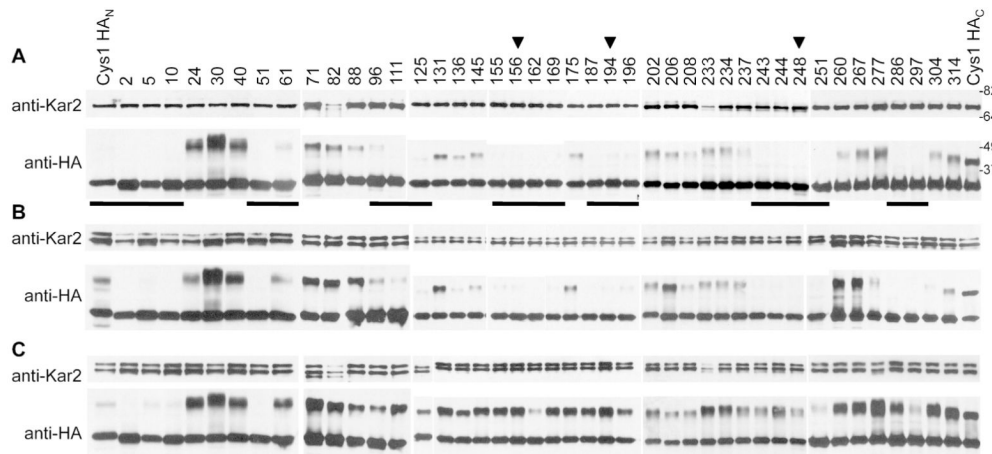


**Figure 4. PEG-Mal accessibility of cysteine-substituted Rce1p mutants**

Microsomes were prepared from yeast EG123 expressing the indicated Rce1p variant and processed according to methods described in Figure 1E, except that the immunoblots were probed using both anti-Kar2p (top panels) and anti-HA antibodies (lower panels). The microsomes were isolated under conditions such that membrane integrity was **A**) preserved (i.e. dounce homogenization), **B**) disrupted by mechanical agitation (i.e. bead beating), or **C**) disrupted by detergent (0.5% Triton X-100). The samples described in **panels A and C** originate from the same population of intact microsomes; the sample was split and treated with PEG-Mal in the absence and presence of detergent. In some instances, PEGylated mutants have differing mobility (e.g. 136 and 145; 304 and 314; *etc.*). The shifts are reproducible across replicates on different gels. The mobility differences are not due to differences in amino acid content since the unmodified species migrate identically to one another. The plasmids used are described in Tables 1 and S1.

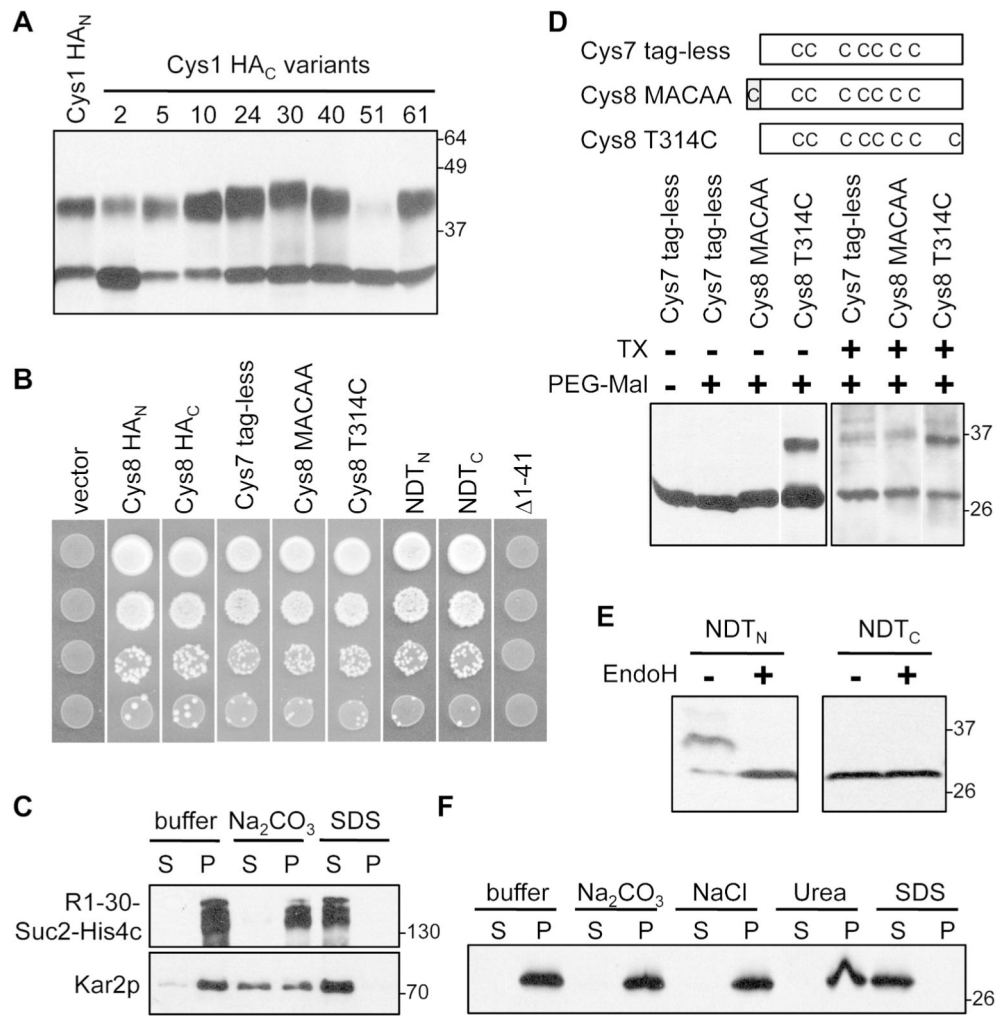


**Figure 5. Analysis of the NH<sub>2</sub> and COOH-termini of Rce1p**

**A**) Microsomes were prepared from yeast EG123 expressing the indicated Rce1p variant and processed according to methods described in Figure 1E in the presence of SDS as it allows for better chemical accessibility to certain cysteine residues. The plasmids used are described in Tables 1 and S1. **B**) Low-copy plasmids encoding the indicated Rce1p variant were evaluated for their ability to confer yeast mating according to the assay described in Figure 2B. Cys8 HA<sub>N</sub> and Cys8 HA<sub>C</sub> contain a triply iterated HA epitope tag at the NH<sub>2</sub> or COOH terminus, respectively, of wildtype Rce1p. Cys7 tag-less contains an Asp-Leu COOH-terminal extension to the otherwise wildtype Rce1p sequence; the extension is a byproduct of the cloning strategy used to eliminate the triply iterated HA tag from the expression vector. Cys8 MACAA contains the Ala-Cys-Ala-Ala sequence inserted after the initiating Met of the Cys7 tag-less Rce1p sequence. Cys8 T314C is a point mutant that introduces a cysteine residue near the COOH terminus of Cys7 tag-less Rce1p. NDT<sub>N</sub> and NDT<sub>C</sub> correspond to variants in which the most distal HA repeat within the triply iterated tag of Cys8 HA<sub>N</sub> and Cys8 HA<sub>C</sub>, respectively, was replaced with a short N-linked glycosylation recognition sequence. Δ1-41 lacks the first 41 amino acids of Cys8 HA<sub>C</sub> and initiates at Met42. The plasmids used were pRS316 (vector), pWS108 (Cys8 HA<sub>C</sub>), pWS1110 (Δ1-41), pWS1146 (Cys8 HA<sub>N</sub>), pWS1157 (Cys7 tag-less), pWS1159 (Cys8 MACAA), pWS1160 (Cys8 T314C), pWS1162 (NDT<sub>N</sub>), and pWS1163 (NDT<sub>C</sub>). **C**) To

probe the nature of R1-30-SUC2-HIS4c membrane association, microsomes were incubated under the indicated conditions (Buffer S, 0.1 M Na<sub>2</sub>CO<sub>3</sub>, or 0.5% SDS), and the soluble (S) and particulate (P) fractions recovered by centrifugation were analyzed by SDS-PAGE and immunoblot. The immunoblot was separately probed with anti-HA (top) and anti-Kar2p (bottom) antibodies. The microsomes were prepared from yeast EG123 transformed with pWS499. **D**) To exclude that the HA tag affects the topology of wild-type Rce1p, high-copy tag-less versions of Rce1p were treated with PEG-Mal in the presence and absence of Triton X-100 (TX), and the immunoblot was probed with anti-Rce1p antibody according to methods described in Figure 1E. Plasmids used were pWS1130 (Cys8 T314C), pWS1131 (Cys8 MACAA), and pWS1158 (Cys7 tag-less). **E**) The indicated NDT variants were evaluated for their sensitivity to EndoH using whole cell extracts. **F**) To probe the nature of 1-41 membrane association, microsomes were incubated under the indicated conditions as in **panel C** and the immunoblot was probed with anti-HA. The microsomes were prepared from yeast EG123 transformed with pWS1110.

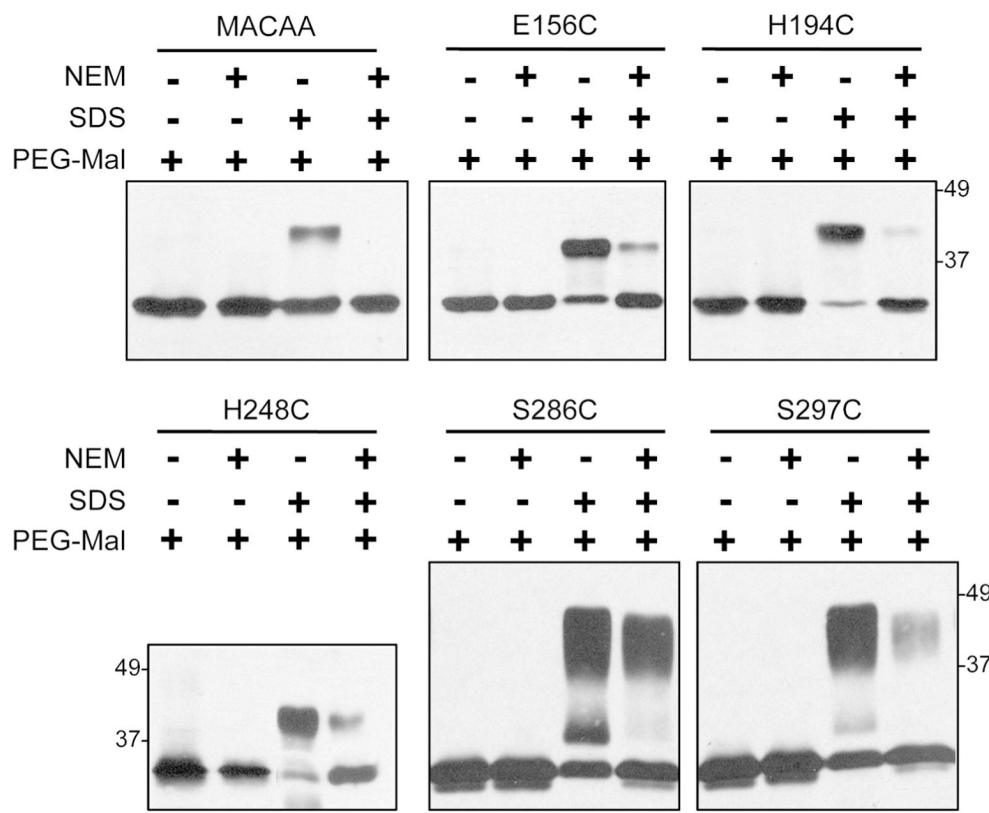


**Figure 6. PEG-Mal accessibility of putative active-site positions after NEM pretreatment**  
 Intact microsomes were prepared from yeast EG123 expressing the indicated Rce1p-HAc Cys0 variant and processed according to methods described in Figure 1E, except that a portion of the sample was pretreated with NEM prior to the PEG-Mal reaction. In some cases, extra bands are observed in the presence of SDS (e.g. S286C and S297C) that appear to be degradation products of the primary PEG-Mal modified species. The plasmids used were pWS970 (S297C), pWS1005 (286C), pWS1012 (E156C), pWS1013 (H194C), pWS1014 (H248C), and pWS1121 (MACAA).

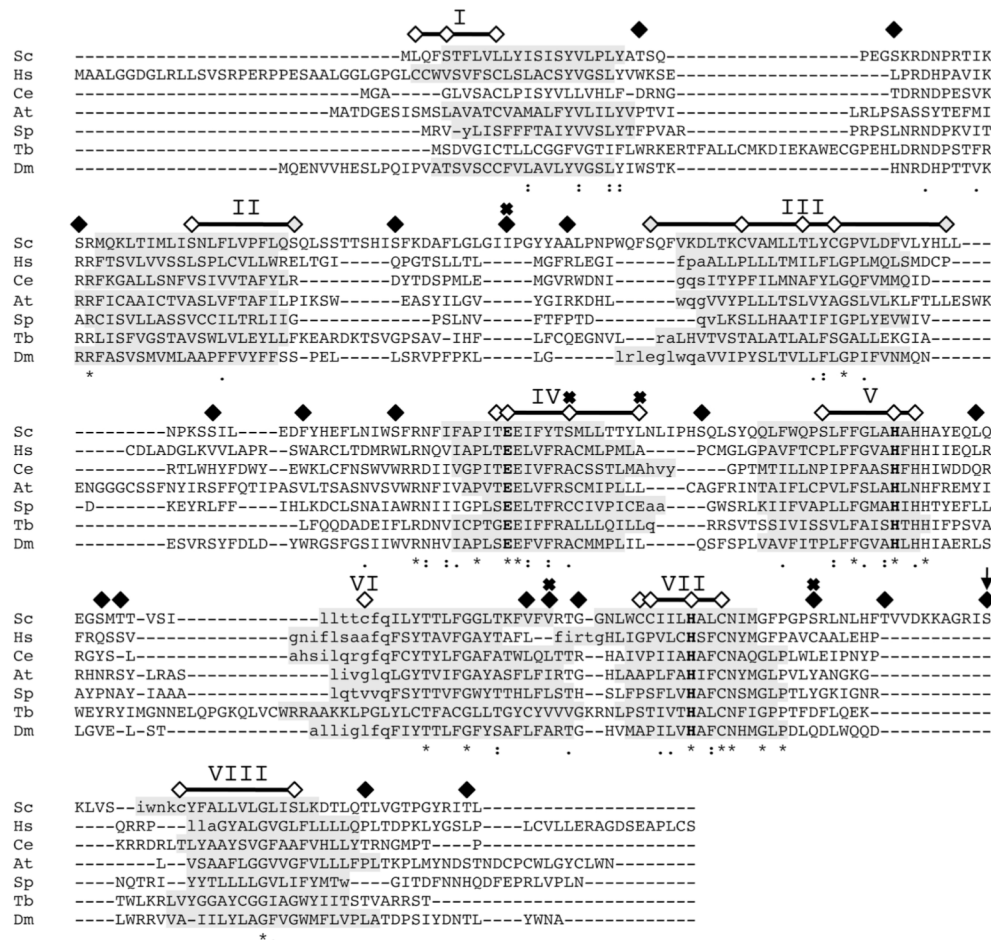


**Figure 7. Multiple sequence alignment and transmembrane segment predictions**

The indicated Rce1p orthologs were aligned using Clustal Omega (*Sc* – *S. cerevisiae*; *Hs* – *H. sapiens*; *Ce* – *C. elegans*; *At* – *A. thaliana*; *Sp* – *S. pombe*; *Tb* – *T. brucei*; *Dm* – *D. melanogaster*). A standard consensus line is shown below the alignment, which indicates invariable (\*), highly conserved (:), and moderately conserved positions (.). Proposed active-site residues are in bold. The residues of *Sc*Rce1p that were non-reactive, weakly reactive and reactive with PEG-Mal are indicated above the yeast sequence (open, grey and closed diamonds, respectively). The position of the 1-277 truncation is marked with an arrow. Mutations that reduced Rce1p activity, other than mutations of proposed active-site residues, are marked with an X above the appropriate diamond. The predicted transmembrane segments of each ortholog, as determined using MEMSAT-SVM are shown with grey background. When a gap adjustment was present within a predicted transmembrane segment, the two split sequences of the predicted segment were spliced together to form an uninterrupted sequence by repositioning the gap adjustment to the nearest edge of the predicted segment. The shorter of the two sequences that were spliced is shown in lower case.

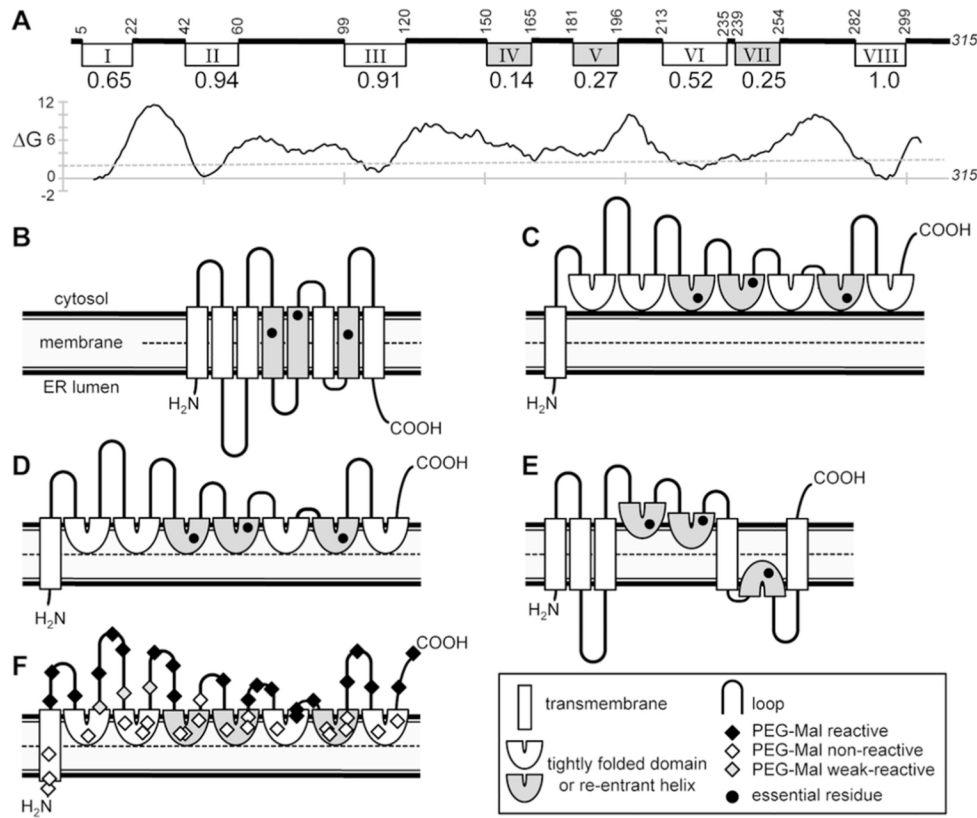


**Figure 8. Topology models**

**A**) Linear representation of yeast Rce1p domains. Arabic numbers reflect amino acid positions determined to lie at the margins of predicted hydrophobic segments (boxes) as defined using MEMSAT-SVM and the wildtype yeast Rce1p sequence; see Figure 7 for detailed sequence information. Roman numerals identify predicted hydrophobic segments. The numbers below the boxes represent a relative predictive score for a transmembrane helix as reported by MEMSAT-SVM. The scores are normalized to the span having the best potential for a transmembrane helix (segment VIII; score 1.0). The segments with relative scores below 0.5 are shaded grey. The graph shows the predicted free energy ( $\Delta G_{app}$ ) for insertion of a 19-residue transmembrane helix centered at the indicated position as reported using G-scale (<http://topcons.cbr.su.se/>) (61). **B-E**) Potential topological arrangements of yeast Rce1p. Pros and cons for each model are discussed in the text. The closed circles represent the approximate position of proposed active-site residues E156, H194 and H248. Each model assumes that segment I is a transmembrane segment. Segments II-VIII are assumed to be **B**) transmembrane segments, **C**) tightly folded cytosolic domains, **D**) re-entrant loops that only enter the cytosolic leaflet of the membrane, or **E**) a combination of all three features. **F**) The model shown in **Panel D** superimposed with PEG-Mal accessibility results derived using intact microsomes from all experiments reported in this study. The data points reflect both natural and introduced cysteine residues. Residues that were non-reactive, weakly reactive and reactive with PEG-Mal are open, grey and closed diamonds, respectively.

**Table 1**  
**Plasmids used in this study**

Plasmid	Genotype	Reference
pJK90	$2\mu URA3 P_{TPI} OST4-HA-SUC2-HIS4c$	(38)
pRS202	$2\mu URA3$	(60)
pRS316	<i>CEN URA3</i>	(60)
pRS416	<i>CEN URA3</i>	(60)
pRS426	$2\mu URA3$	(60)
pWS100	<i>CEN URA3 RCE1</i> (alias pSM1275)	(3)
pWS108	<i>CEN URA3 RCE1-HA<sub>C</sub></i> (alias pSM1314)	(3)
pWS127	$2\mu URA3 P_{PGK}-His_{10}-HA_N-RCE1 (L177I)$	this study
pWS398	<i>CEN URA3 RCE1-HA<sub>C</sub> (C251A)</i>	(5)
pWS404	$2\mu URA3 RCE1-HA_C$	(5)
pWS492	<i>CEN URA3 RCE1-HA<sub>C</sub> Y22A</i>	(5)
pWS499	<i>CEN URA3 P<sub>TPI</sub>-RCE1 (1-30)-HA-SUC2-HIS4<sub>C</sub></i>	this study
pWS566	$2\mu URA3 P_{PGK}-RCE1 (1-277)-HA-10HIS_C$	this study
pWS787	<i>CEN URA3 RCE1-HA CysO</i>	this study
pWS822	$2\mu URA3 RCE1-HA_C CysO (C354)$	this study
pWS823	$2\mu URA3 RCE1-HA CysO$	this study
pWS934	$2\mu URA3 P_{PGK}-His_{10}-HA_N-RCE1-HA CysO$	this study
pWS954	$2\mu URA3 RCE1-HA (C354S)$	this study
pWS955	<i>CEN URA3 RCE1-HA (C354S)</i>	this study
pWS1005	$2\mu URA3 RCE1-HA_C CysO (C286)$	this study
pWS1074	<i>CEN URA3 RCE1-HA (F234C)</i>	this study
pWS1097	<i>CEN URA3 RCE1-HA (S162C)</i>	this study
pWS1110	<i>CEN URA3 RCE1-HA<sub>C</sub> (I-4I)</i>	this study
pWS1119	<i>CEN URA3 RCE1-HA<sub>C</sub> (MACAA)</i>	this study
pWS1121	$2\mu URA3 RCE1-HA_C CysO (MACAA)$	this study
pWS1126	$2\mu URA3 RCE1-HA_C (MACAA)$	this study
pWS1127	<i>CEN URA3 RCE1-HA<sub>C</sub> CysO (MACAA)</i>	this study
pWS1130	$2\mu URA3 RCE1 (T314C)-DL$	this study
pWS1131	$2\mu URA3 RCE1 (MACAA)-DL$	this study
pWS1146	<i>CEN URA3 His<sub>10</sub>-HA<sub>N</sub>-RCE1</i>	this study
pWS1157	<i>CEN URA3 RCE1-DL</i>	this study
pWS1158	$2\mu URA3 RCE1-DL (Cys7 tag-less)$	this study
pWS1159	<i>CEN URA3 RCE1 (MACAA)-DL</i>	this study
pWS1160	<i>CEN URA3 RCE1 (T314C)-DL</i>	this study
pWS1162	<i>CEN URA3 NDT-HA<sub>N</sub>-RCE1</i>	this study
pWS1163	<i>CEN URA3 RCE1-HA<sub>C</sub>-NDT</i>	this study
pWS1167	$2\mu URA3 NDT-HA_N-RCE1$	this study
pWS1168	$2\mu URA3 RCE1-HA_C-NDT$	this study

**Table 2**  
**Summary of PEG-Mal and Hydropathy Analyses of Rcelp**

Method	Segment							
	I	II	III	IV	V	VI	VII	VIII
PEG-Mal	2-10	51-61	96-125	155-169	187-196	217	243-251	286-297
MEMSAT-SVM	5-22	42-60	99-120	150-165	181-196	213-235	239-254	282-299
Predict Protein	5-22	45-62	100-118	147-164	182-199	212-229	234-252	281-299